Electronic Supplementary Material (ESI) for ChemComm.

Supplementary Information for

Directing oligopeptide amphiphile into aligned nanofiber matrix for elucidating molecular structures

Si-Yong Qin,*[a] Wen-Qiang Ding,[a] Zhi-Wei Jiang,[a] Xinxiang Lei,*[a,b] Ai-Qing Zhang*[a]

[a]College of Chemistry and Materials Science, South-Central University for Nationalities, Wuhan 430074, P. R. China.

[b]School of Pharmaceutical Sciences, South-Central University for Nationalities, Wuhan, 430074 (P. R. China).

E-mail: sy-qin@mail.scuec.edu.cn; xxlei@mail.scuec.edu.cn; aizhang@scuec.edu.cn.

Experimental Section

Materials: All the amino acids and coupling reagents used to prepare OPAs were purchased from GL Biochem (Shanghai) Ltd. (China). Palmitic acid (AR) and proline (98% purity) were provided by Aladdin and Macklin, respectively. Raffinose (98% purity) was obtained from Shanghai yuanye Bio-Technology Co., Ltd. Unless noted, all materials were reagent grade and used as received without further purification.

Synthesis of OPAs: Synthesis of OPAs was carried out based on orthogonal Fmoc/Boc solid-phase synthesis method according to the literature.[1] The obtained crude peptides were purified by high-pressure liquid chromatography (HPLC).

OPAs structure characterization: The molecular weight of OPAs was recorded using matrix-assisted laser desorption/ionization time of flight mass spectrometry (MALDI-TOF MS) and electrospray ionization mass spectrometry (ESI-MS, LCQ Advantage, Finigan, USA). The purity of OPAs was measured by high-pressure liquid chromatography (HPLC, LC-20AR, Shimadzu, Japan) equipped with a C18 column (SinoChrom ODS-BP, 4.6*250 mm, 5 μm). Solvent A (acetonitrile containing 0.1% trifluoroacetic acid) and B (water containing 0.1% trifluoroacetic acid) were used as the eluting agents, and the linear gradient begun with 48% of A and 52% of B. The components were collected at the wavelength of 220 nm.

Self-assembled secondary conformation characterization: Fourier-transform infrared (FT-IR) spectra of the lyophilized OPA nanofibers were acquired on IRTracer-100. Prior to the measurement, the samples were pressed into pellet with

KBr powder. Circular dichroism (CD) was recorded on a Chirasca^{TM}-plus Circular Dichroism Spectrometer (Applied Photophysics). 1 wt % OPA1 solution was poured into a 1 mm quartz cell and analyzed with 4 s accumulations every 1 nm and averaged over five acquisitions. The data was collected from 185 nm to 250 nm. As for the heating and cooling cycles, 1 ^{o}C/min rate was set.

Nanofiber preparation and heating-enhanced alignment: To prepare OPA1 nanofibers, a certain amount of OPA1 was weighed out and dH_2O was added to disperse it. 1.0 M NaOH was dropped into the suspension to adjust pH value to ~7, as a result of a translucent solution. To obtain the aligned oligopeptide nanofiber fluid, OPA1 with concentration of 10 wt% was used, which was heated to 80 ^{o}C and kept at this temperature for 2 h before cooling to room temperature.

SEM characterization: Scanning electron microscopy (SEM) images of self-assembled OPA1 nanofibers at low concentration of 0.1 wt% were obtained on a Nova NanoSEM FEI (Holland) instrument with an accelerating voltage of 30 kV. OPA solution was dropped onto a glass substrate and dried in air, which was further dehydrated under vacuum. Then the sample was coated with gold for the observation. To investigate the microstructure of OPA1 nanofibers at high concentration of 10% wt, the samples were dried by a supercritical dryer (SAMDRI®-PVT-3D). Briefly, water was slowly exchanged with ethanol until the solution was 100% ethanol. Then, the samples were located in supercritical dryer and ethanol was exchanged with liquid CO_2, followed by the heating for the gasification of CO_2. After coated by gold, the samples were then imaged on a Zeiss Gemini 300 microscope.

TEM characterization: Transmission electronic microscopy **(**TEM) image of self-assembled nanofiber at concentration of 0.1 wt% was obtained (TEM, JEOL-2100, Japan). The TEM sample was prepared by dipping a copper grid into the oligopeptide solution. After the deposition, the sample was dried in air.

ζ-Potential Measurement: The ζ-potential of OPA1 nanofiber solution with a concentration of 0.1 wt% was measured with Nano-ZS ZEN3600 (Malvern Instruments) at 25 ^{o}C.

Wide-Angle X-ray Diffraction (WXRD): The WXRD pattern of lyophilized OPA1 nanofiber was recorded by a Shimadzu XRD-6000 diffractometer with a Ni filter and Cu $K_{\alpha 1}$ (λ=1.54056 Å, I=40 mA and V=40 kV). Before the scanning, the supramolecular nanofiber powder was spread on glass slides.

Polarized Optical Microscopy (POM): POM experiments were performed by placing the OPA1 fluid sample between crossed polarizers in polarized microscope (Nikon Eclipse Lv100npol). OPA1 with 10 wt% used and spread out on a glass slide.

Small Angle X-Ray Scattering (SAXS): SAXS investigation was performed in Shanghai Synchrotron Radiation Facility, using a fixed wavelength of 1.023 nm. The sample-detector distance is 2717 mm, and detector pixel size is 172 μm, with an exposure time of 1 s. The scattering intensity was recorded in the interval $0.007 < q < 0.29$ A^{-1}. All data were analyzed and processed using RAW. For the temperature-dependent measurements, samples were sealed within 1.5 mm quartz capillaries that were placed in a Linkum THMS thermo stage. The samples were heated at a rate of 4

°C/min and held for 2 h at different temperatures. The 2D SAXS images were azimuthally averaged to produce one-dimensional profiles of intensity, I vs. q, using the two-dimensional data reduction program FIT2D. The scattering spectra of the capillary and solvent (water) were also collected and subtracted from the corresponding solution data.

NMR analysis: All ^{1}H NMR spectra of OPA1 with different concentrations were measured at 20 °C on a Bruker AVANCE III 600-MHz spectrometer equipped with a BBO cryogenic Prodigy probe with z-gradients. All ^{2}H NMR data were obtained on a Bruker Avance III NMR spectrometer (600.11 MHz for ^{1}H NMR; 92.12 MHz for ^{2}H NMR; 150.91 MHz for ^{13}C NMR, respectively) equipped with a 5-mm BBO Prodigy cryo-probe, BB-(H-F)-D-05-Z (Bruker Instruments Inc., Germany) at 293 K. The ^{2}H NMR acquisition was recorded using the lock channel. For the [^{1}H,^{13}C]-CLIP-HSQC spectra, the conditions were as follows: acquisition time (AQ) 0.327 s, relaxation delay (RD) 2.00 s, and spectral width (SW) 10 ppm for ^{1}H and 140 ppm for ^{13}C. A total of 4 k data points were sampled in the direct dimension over a spectral width of 10 ppm. A one-bond coupling constant was 145.0 Hz. LB 1Hz for F2 and 0.3 Hz for F1 were applied before Fourier transformation.

REFERENCES

1. Qin, S. Y.; Peng, M. Y.; Rong, L.; Jia, H. Z.; Chen, S.; Cheng, S. X.; Feng, J.; Zhang, X. Z. An innovative pre-targeting strategy for tumor cell specific imaging and therapy. Nanoscale **2015**, *7*, 14786–14793.

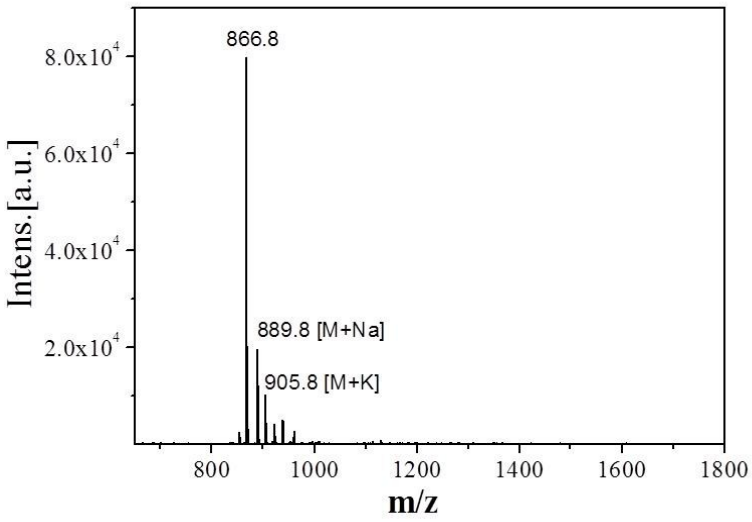

Fig. S1. MALDI-TOF MS of OPA1. M at m/z 866.8, [M+Na] at 889.8, and [M+K] at 905.8 were observed.

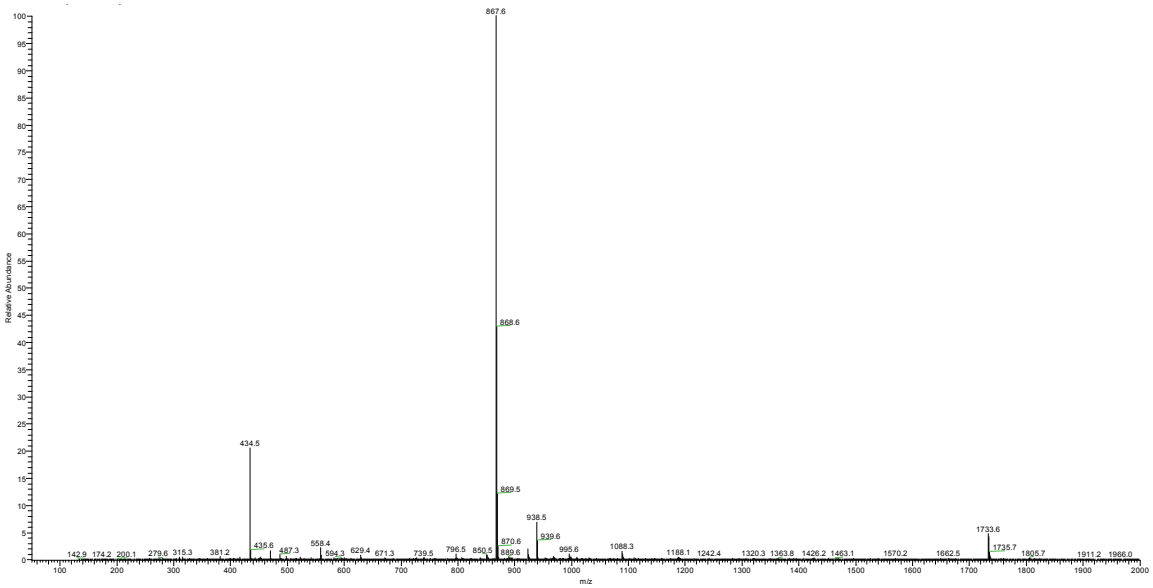

Fig. S2. ESI-MS of OPA1. $[M+H]^+$ at m/z of 867.6 and $[M+2H]^{2+}/2$ at 434.5 were observed.

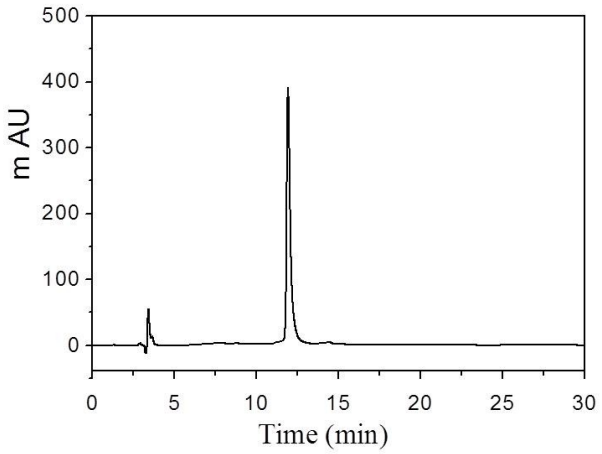

Fig. S3. HPLC profile of OPA1, with a purity of 95.6%.

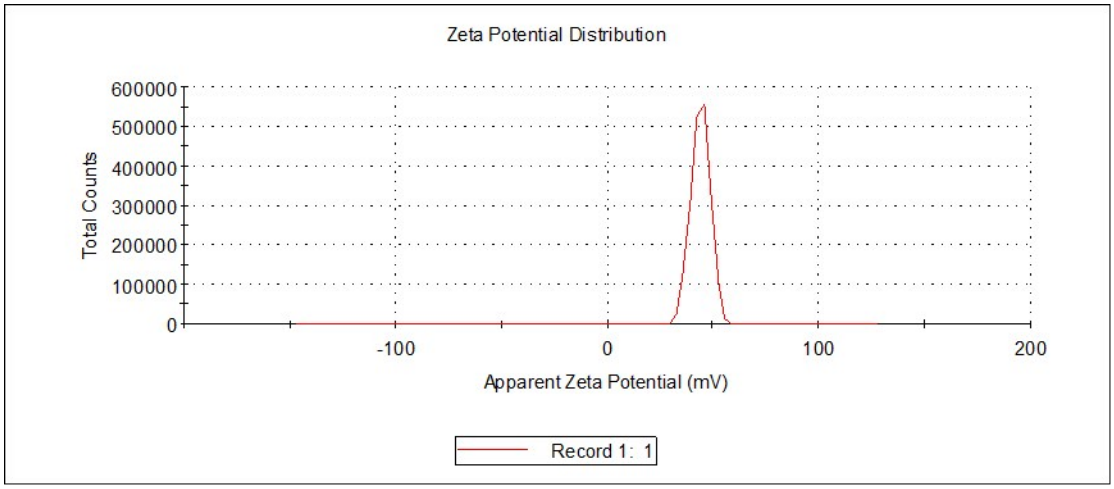

Fig. S4. ζ-potential of OPA1 solution (0.1 wt%).

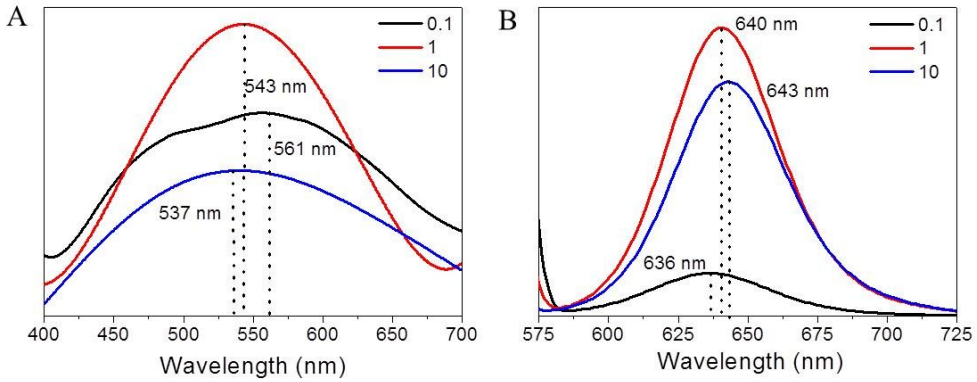

Fig. S5. (A) UV-vis and (B) fluorescence emission spectra of Nile red in OPA1 solutions with different concentrations. The excitation wavelength of fluorescent emission spectra is 550 nm. Along with elevating the OPA1 concentration, a blue-shift from 561 to 537 nm in UV-vis absorption and a red-shift from 636 to 643 nm in fluorescence spectra were observed, respectively.

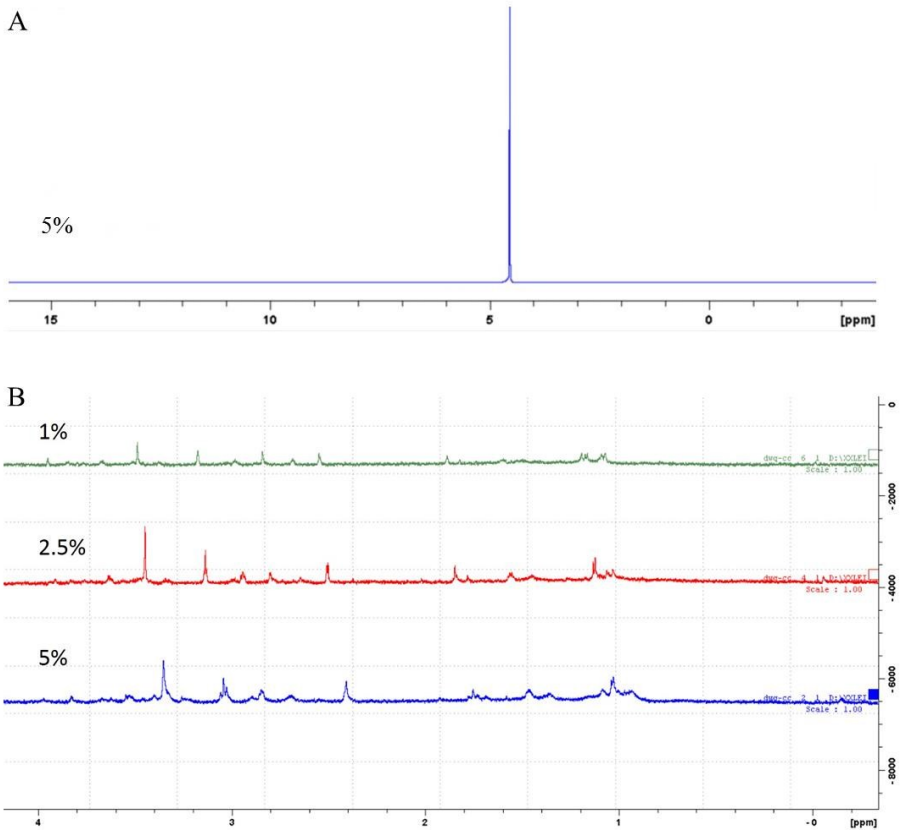

Fig. S6. ^{1}H NMR of OPA1 with different concentrations (D_2O). (A) ^{1}H NMR spectrum of OPA1 only showing a solvent signal even at 50 mg/mL, indicating the formation of supramolecular aggregate. (B) ^{1}H NMR spectra of OPA1 after the solvent signal was suppressed by presaturation with 64 scans. The chemical shifts of alkyl chain protons showed an upfield shift along with elevating the OPA1 concentration, suggesting the participation of hydrophobic interaction. Meanwhile, the signal intensity did not follow the principle that NMR signal intensity depends on molar concentration and related to square root of scans of numbers ($n^{1/2}$), suggesting the stronger molecular interactions at higher concentrations.

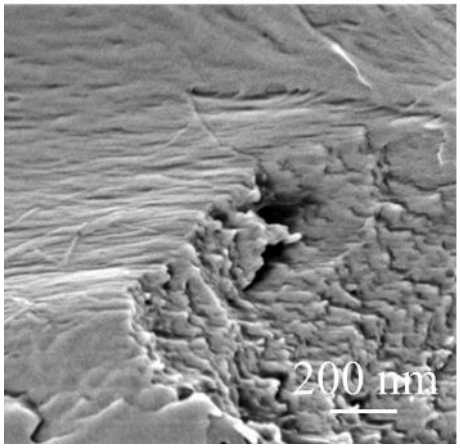

Fig. S7. SEM image of cross-section of self-assembled nanofibers.

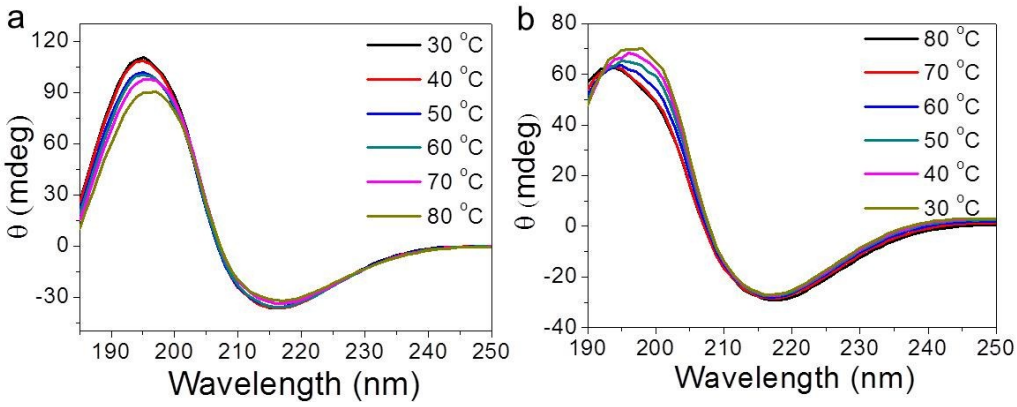

Fig. S8. Variable-temperature CD of 1 wt% OPA1 solution during the heating (a) and cooling (b).

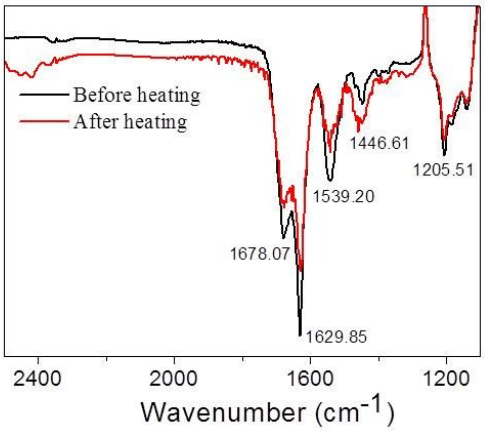

Fig. S9. FT-IR spectra of the freeze-dried nanofibers with and with heating treatments.

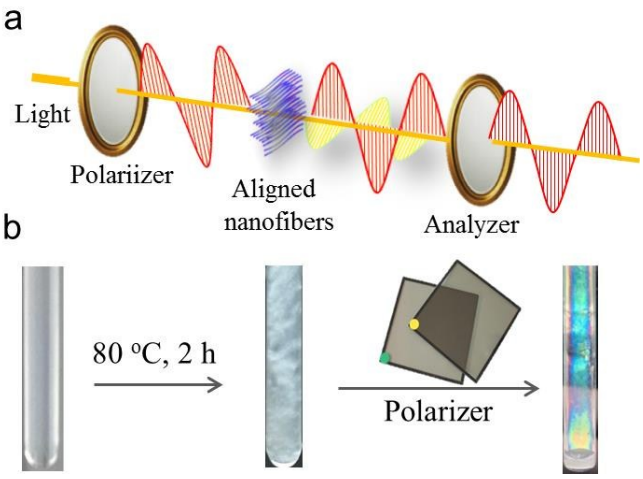

Fig. S10. (a) Schematic illustration for the detection of laser power passed through the aligned nanofiber fluid. (b) Photographs of self-assembled nanofiber fluid in an NMR tube before and after heating, and its birefringent image between two polarizers.

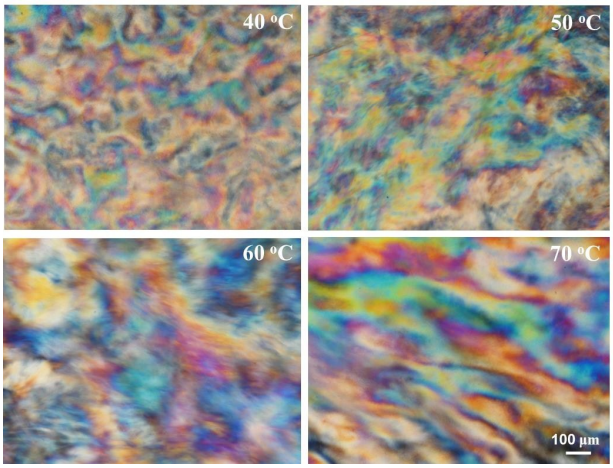

Fig. S11. POM images of OPA1 fluid (10 wt%) after heating at different temperatures.

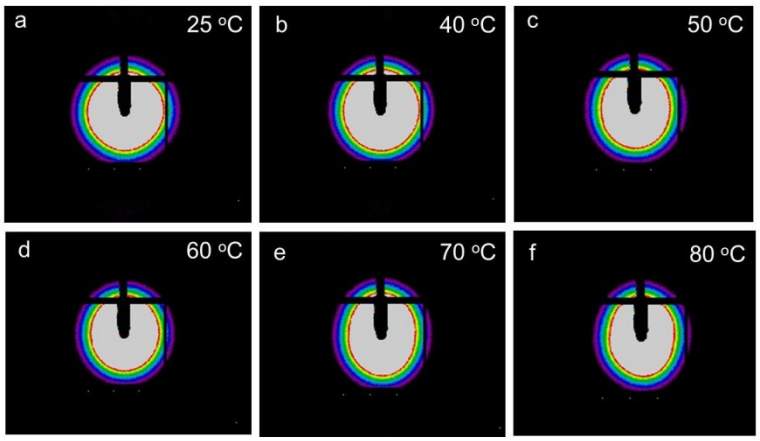

Fig. S12. 2D SAXS of OPA1 fluid after heating at different temperatures for 2 h.

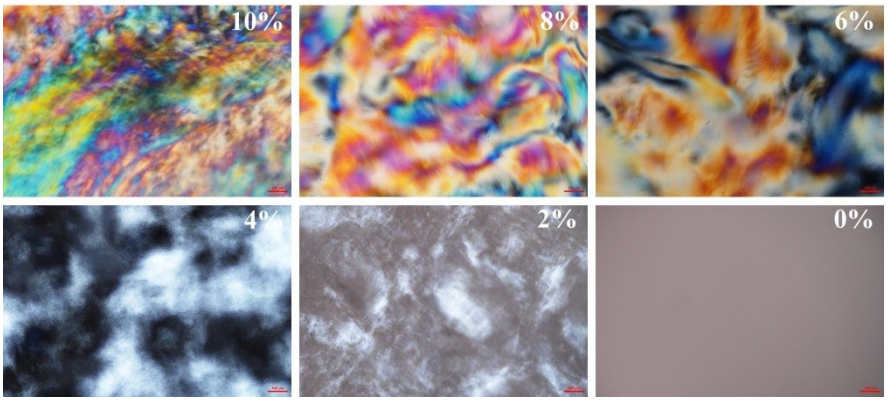

Fig. S13. POM images of OPA1 fluid with different concentrations after heating.

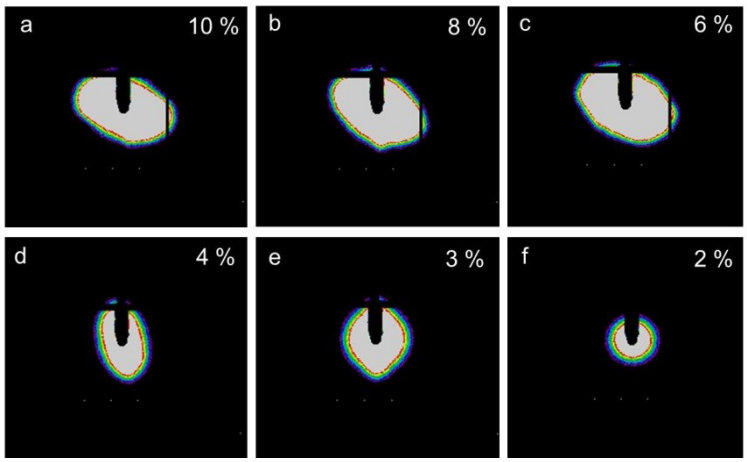

Fig. S14. 2D SAXS of the heated OPA1 fluid with different concentrations.

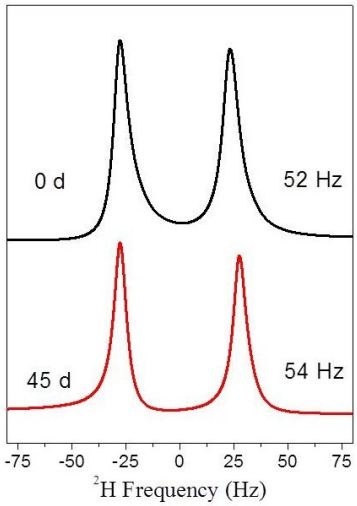

Fig. S15. 1D 2H spectra (92.1 MHz) of self-assembled nonofibers matrix at different time intervals.

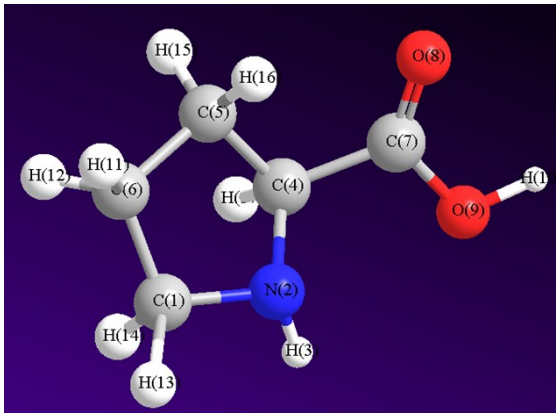

Fig. S16. 3D structure and atomic number of proline.

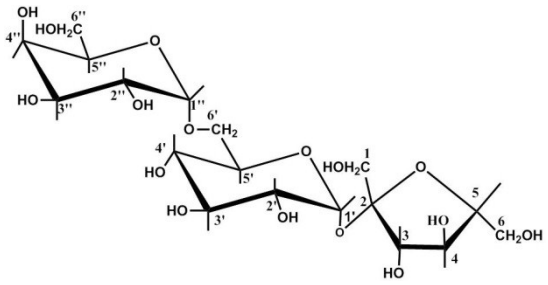

Fig. S17. Chemical structure of raffinose.

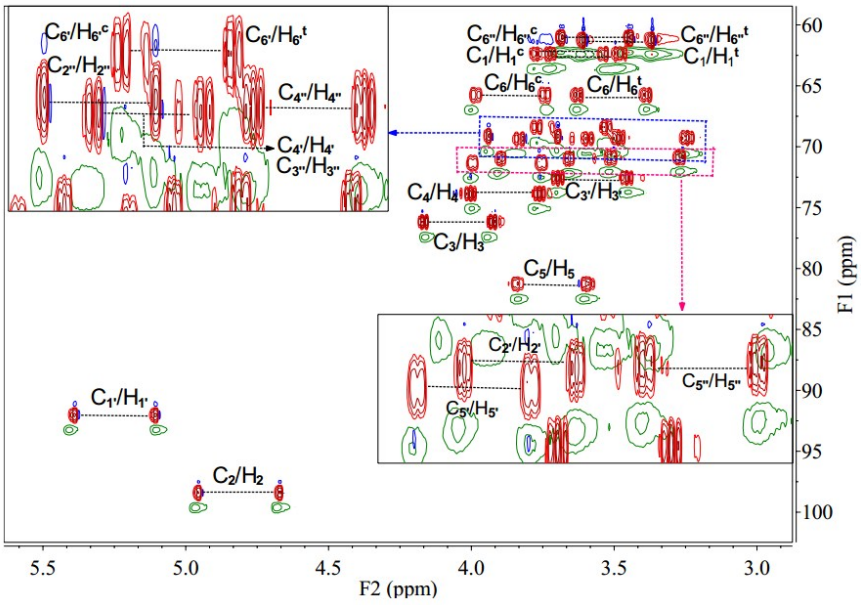

Fig. S18. CLIP-HSQC spectrum of raffinose in the isotropic D2O phase (red) and in anisotropic OPA1 nanofiber fluid (green).

Table S1. Oligopeptide Amphiphiles (OPAs) investigated to construct the aligned nanofibers.

OPAs	Sequence	Molecular weight	Solubility	POM	RQC (Hz)
OPA1	$C_{15}H_{31}CO$-AAAAAKK-$CONH_2$	867	pH 7-8	Yes	82
OPA2	$C_{15}H_{31}CO$-AAAAKKK-$CONH_2$	925	Easy to dissolve	No	0
OPA3	$C_{15}H_{31}CO$-VVVVKKK-$CONH_2$	1036	Easy to dissolve	No	0
OPA4	$C_{15}H_{31}CO$-AAAAAEE-$CONH_2$	869	pH>9	Yes	6
OPA5	$C_{15}H_{31}CO$-AAAAAEE-COOH	870	pH>9	No	0
OPA6	$C_{15}H_{31}CO$-AAAAAEEE-$CONH_2$	1016	pH>9	No	0
OPA7	$C_{15}H_{31}CO$-AAAAASS-$CONH_2$	783	Insoluble	No	0
OPA8	$C_{15}H_{31}CO$-AAAAAKEEE-$CONH_2$	1162	Easy to dissolve	Yes	0
OPA9	$C_{15}H_{31}CO$-AAAAAKKEEE-$CONH_2$	1308	Easy to dissolve	Yes	0

Table S2. Carbon-13 chemical shifts of raffinose in D2O (ppm)

	1	2	3	4	5	6
fructofuranose	62.36	98.21	76.40	74.23	81.54	65.92
glucopyranosyl	91.88	70.50	72.23	69.33	71.64	66.60
galactopyranosyl	95.59	69.15	69.33	69.28	70.64	60.81

Table S3. $^{1}D_{CH}$ values of raffinose in aligned nanofiber fluid.

Atom number	$^{1}J_{CH}$ (Hz)	$^{1}T_{CH}$ (Hz)	RDCs (Hz)	Atom number	$^{1}J_{CH}$ (Hz)	$^{1}T_{CH}$ (Hz)	RDCs (Hz)
C_1/H_1^c	173.21	182.99	9.78	C_4'/H_4'	145.20	163.63	18.43
C_1/H_1^t	148.83	193.23	44.40	C_5'/H_5'	154.44	148.33	-6.11
C_2/H_2	170.80	157.20	-13.60	$C_6'/H_6'^c$	39.56	25.47	-14.09
C_3/H_3	144.07	129.58	-14.49	$C_6'/H_6'^t$	147.13	127.90	-19.23
C_4/H_4	154.76	129.29	-25.47	C_2''/H_2''	173.52	183.31	9.79
C_5/H_5	149.29	134.63	-14.66	C_3''/H_3''	145.20	163.63	18.43
C_6/H_6^c	145.23	156.28	11.05	C_4''/H_4''	144.99	161.34	16.35
C_6/H_6^t	144.15	148.08	3.93	C_5''/H_5''	143.69	161.34	17.65
C_1'/H_1'	174.74	182.98	8.24	$C_6''/H_6''^c$	143.79	145.53	1.74
C_2'/H_2'	143.17	154.21	11.04	$C_6''/H_6''^t$	144.68	146.95	2.27
C_3'/H_3'	144.98	156.23	11.25				